

ОБЪЕДИНЕННЫЙ  
ИНСТИТУТ  
ЯДЕРНЫХ  
ИССЛЕДОВАНИЙ

Дубна

E1-2005-131

J. Adelman<sup>1</sup>, J.-F. Arguin<sup>2</sup>, G. Bellettini<sup>3</sup>, E. Brubaker<sup>1</sup>, J. Budagov<sup>4</sup>,  
G. Chlachidze<sup>4</sup>, L. Demortier<sup>5</sup>, A. Gibson<sup>6</sup>, S. Kim<sup>7</sup>, Y.-K. Kim<sup>1</sup>,  
T. Maruyama<sup>7</sup>, K. Sato<sup>7</sup>, M. Shochet<sup>1</sup>, P. Sinervo<sup>2</sup>, T. Tomura<sup>7</sup>,  
G. Velev<sup>8</sup>, S. Xie<sup>2</sup>, U.-K. Yang<sup>1</sup>

(On behalf of the CDF Collaboration)

MEASUREMENT OF THE TOP QUARK MASS  
USING THE TEMPLATE METHOD  
IN THE LEPTON PLUS JETS CHANNEL  
WITH IN SITU  $W \rightarrow jj$  CALIBRATION AT CDF-II

<sup>1</sup> Enrico Fermi Institute, University of Chicago, USA

<sup>2</sup> University of Toronto, Canada

<sup>3</sup> INFN, Pisa, Italy

<sup>4</sup> JINR, Dubna, Russia

<sup>5</sup> Rockefeller University, USA

<sup>6</sup> Lawrence Berkeley Laboratory, USA

<sup>7</sup> University of Tsukuba, Japan

<sup>8</sup> Fermi National Accelerator Laboratory, USA

2005



## 1. INTRODUCTION

The direct observation of the top quark in 1995 [1] was not a big surprise since the  $b$  quark is expected to have a isospin partner to insure the viability of the Standard Model. What was surprising at the time of the discovery was its large mass, almost 35 times the mass of the  $b$  quark. The top quark mass is a fundamental parameter of the Standard Model, and plays an important role in the precise prediction of electroweak observables like the Higgs boson mass. Indeed, the radiative corrections of many electroweak observables are dominated by the large top quark mass. Furthermore, a large value of the top quark mass indicates a strong Yukawa coupling to Higgs, and could be a sign for a special role of the top quark in the understanding of electroweak symmetry breaking [2]. Thus, a precise measurement of the top quark mass provides a crucial test of the consistency of the Standard Model and could help constraining physics beyond the Standard Model. In this paper, we report on a measurement of the top quark mass with the CDF-II detector, using the data sample from March 2002 to August 2004 runs, corresponding to a total integrated luminosity of  $318 \text{ pb}^{-1}$  data.

At the Tevatron, top quarks are produced primarily as top pairs and decay to  $W$  bosons and  $b$  quarks nearly 100% of the time within the Standard Model. Then, the  $W$  bosons can decay into lepton-neutrino ( $l\nu$ ) or quark pairs ( $q\bar{q}$ ). In this measurement, we use the «lepton + jet» channel of  $t\bar{t}$  candidates in which only one of two  $W$  bosons decays to  $l\nu$  while the other decays to quark pairs.

This analysis uses the CDF detector to identify and reconstruct the  $t\bar{t}$  events. CDF is a multipurpose collider detector made of silicon detectors near the interaction point to measure the primary vertex position and provide high-efficiency  $b$ -tagging. The next detector in increasing radius from the beamline is the Central Outer Tracker (COT), an open-cell drift chamber that provides high precision charged particles tracking. The CDF tracking system is embedded in a superconducting solenoid that provides a uniform magnetic field of 1.4 T. Behind the solenoid there are located electromagnetic and hadronic sampling calorimeters that have the primary task to detect electrons, photons and jets as well as to measure the transverse missing energy ( $\cancel{E}_T$ ) induced by the presence of neutrinos. The muon identification is performed by a set of detectors located behind the calorimeters that are made of wire chambers and layers of steel. A complete description of the CDF detector is provided elsewhere [3].

## 2. EVENT SELECTION

The lepton+jets events are selected by requiring one well-identified electron or muon, large ( $\cancel{E}_T$ ) due to the neutrino from the  $W$  decay and at least four jets in the final state. Electron candidates are identified as a high-momentum track

in the tracking system matched to an electromagnetic cluster reconstructed in the calorimeters with  $E_T > 20$  GeV. The shower lateral and longitudinal profile of the cluster is required to be consistent with the one of an electromagnetic shower. Muon candidates are reconstructed as high-momentum track with  $p_T > 20$  GeV/ $c$  with matching hits in the muon chambers. The missing transverse energy is measured by the imbalance in the calorimeter transverse energy and is required to be greater than 20 GeV. Jets are reconstructed with the JETCLU cone algorithm with a radius  $R = \sqrt{\eta^2 + \phi^2} = 0.4$ . At least 4 jets are required with the jet  $E_T$  requirement depending on the event category as described below. A final requirement is applied only for the top quark mass reconstruction: the minimized  $\chi^2$  value from the kinematic fit described in Sec. 4 is required to be  $< 9$ . This requirement is not applied for the  $W$  boson mass reconstruction since it reduces the sensitivity of this observable to the jet energy scale.

To improve the statistical power of the method, the lepton + jets sample is divided into four subsamples with various sensitivity to the top quark mass. First, the events are separated based on the number of jets that are  $b$ -tagged in the event. The SECVTX algorithm [5] based on the identification of secondary vertices inside jets is used to tagged  $b$ -jets. Events with 2-, 1- and 0-tag are considered separately. Indeed, events with increasing number of  $b$ -tags have better mass resolution (as described in Sec. 4) and lower background contamination (as described in Sec. 6). Furthermore, events with 1-tag are separated based on the 4th jet  $E_T$  threshold. Events in the 1-tag(T) category have 4 jets with  $E_T > 15$  GeV, while events in the 1-tag(L) category have 3 jets with  $E_T > 15$  GeV and the 4th jet with  $8 < E_T < 15$  GeV. Events in the 1-tag(T) sample are less contaminated by background. Table 1 describes the four subsamples with their expected signal to background ratio and the number of events observed in data (before and after the  $\chi^2$  cut).

Table 1. Jet  $E_T$  cut and  $b$ -tagging requirement for the 4 event categories. Also is shown the expected signal to background ratio (S:B) for each subsample as well as the number of events observed in data before and after the  $\chi^2$  cut. Note that there is no background estimate yet available for the 0-tag subsample, so the *a priori* S:B is unknown for that category

Category	2-tag	1-tag(T)	1-tag(L)	0-tag
Jet $E_T$ cuts: j1-j3, j4, GeV	$E_T > 15$ $E_T > 8$	$E_T > 15$ $E_T > 15$	$E_T > 15$ $E_T > 8$	$E_T > 21$ $E_T > 21$
$b$ -tagging	2 tags	1 tag	1 tag	0 tag
Expected S:B	10.6:1	3.7:1	1.1:1	N/A
Number of events	25	63	33	44
Number of events with $\chi^2 < 9$	16	57	25	40

### 3. JET ENERGY SCALE UNCERTAINTY

We describe in this section the *a priori* determination of the jet energy scale uncertainty by CDF that is used later in this analysis. There are many sources of uncertainties related to jet energy scale in CDF, i.e., uncertainties in the modeling of the jet response in the Monte Carlo simulation:

- Relative response of the calorimeters as a function of pseudorapidity with respect to the central calorimeter.
- Single particle response with the calorimeters.
- Fragmentation of jets.
- Modeling of the underlying event energy.
- Amount of energy deposited out-of-cone.

The uncertainties of each source are evaluated separately as a function of the jet  $p_T$  (and  $\eta$  for the first uncertainty in the list above). Their contributions are shown in Fig. 1 for the region  $0.2 < \eta < 0.6$ . The black lines show the sum in quadrature of each contribution. This  $\pm 1\sigma$  total uncertainty on the jet energy scale is used as the unit of jet energy scale in this analysis. For instance, the templates of reconstructed top quark mass  $m_t^{\text{reco}}$  and  $W$  boson mass  $m_{jj}$  are constructed for various values of JES in units of  $\sigma$ . Furthermore, this *a priori* information on the jet energy scale is used in the likelihood fit as an additional constraint on JES.

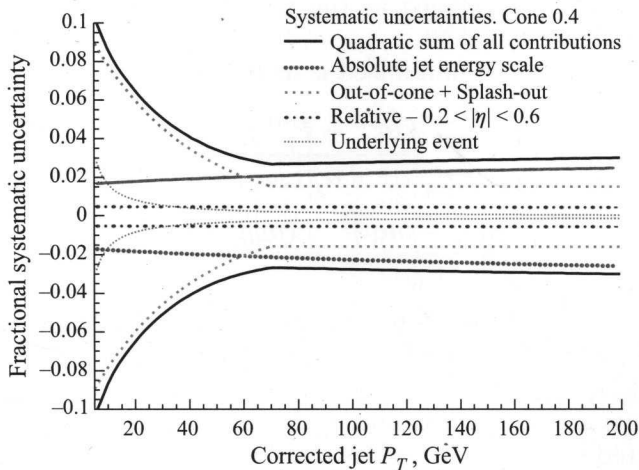


Fig. 1. Jet energy scale uncertainty as a function of the corrected jet  $p_T$  for the underlying event (dotted red), relative response (dashed green), out-of-cone energy (dashed red) and absolute response (dashed blue). The contribution of all sources are added in quadrature (full black)

### 4. TOP QUARK MASS RECONSTRUCTION

For each lepton + jet event, an invariant mass of the top quark is reconstructed from the top decay products (lepton candidate, four highest  $E_T$  jets and missing transverse energy) using a  $\chi^2$  kinematic fit. Reconstructed top quark mass distributions are produced using HERWIG [4] Monte Carlo events for various

true top quark mass and jet energy scale hypothesis. They are called top quark mass templates. These distributions have a strong dependence on the true top quark mass that is then extracted by comparing the reconstructed top quark mass distribution in the data with the various templates using a maximum likelihood fit (described in Sec. 8). As discussed in more detail in the following section, templates of the  $W$  boson dijet mass are also considered.

The  $\chi^2$  kinematic fit is based on the hypothesis that the event of study is signal. The measured three-momenta of the lepton, two  $b$ -jets and two light quark jets are inputs to the  $\chi^2$  fit. The measured momenta of final state particles are further corrected with respect to the event selections such that they correspond as closely as possible to the momenta of the particles directly arising from the top quark decays. The muon momentum is corrected for the residual misalignment of the COT. Jets have their energy corrected for the nonlinear response of single hadronic particles in the CDF calorimeters, energy deposited out of the cone and underlying event energy contributions inside the cone. In addition, flavor specific corrections are applied separately for light quark jets and  $b$ -jets. These corrections use the information of the  $p_T$  spectrum shape of jets in  $t\bar{t}$  events and are  $p_T$ - and  $\eta$ -dependent. The top-specific corrections are constructed such that after all corrections the average jet energy corresponds to the one of the parton that initiated the jet. The unclustered energy represents all the transverse energy in the event that is not due to the lepton or jets in the final state. The transverse energy of the neutrino is defined as the negative sum of the lepton, jets, and unclustered transverse energies.

The  $\chi^2$  expression to be minimized is as follows:

$$\chi^2 = \sum_{i=l,4\text{jets}} \frac{(\hat{P}_T^i - P_T^i)^2}{\sigma_i^2} + \sum_{j=x,y} \frac{(\hat{P}_j^{\text{UE}} - P_j^{\text{UE}})^2}{\sigma_j^2} + \frac{(m_{jj} - m_W)^2}{\Gamma_W^2} + \frac{(m_{l\nu} - m_W)^2}{\Gamma_W^2} + \frac{(m_{bjj} - m_t^{\text{rec}})^2}{\Gamma_t^2} + \frac{(m_{bl\nu} - m_t^{\text{rec}})^2}{\Gamma_t^2}, \quad (1)$$

where  $\sigma_l$  and  $\sigma_{\text{jet}}$  correspond to resolutions of the lepton and four leading jets, and  $p_{x,y}^{\text{UE}}$  and  $\sigma_{x,y}$  are the  $x$  and  $y$  components of the unclustered energy and resolution, respectively. The  $t$  and  $\bar{t}$  masses are constrained to be the same, and the two  $W$  masses are both constrained to be the PDG value of  $M_W = 80.42$  GeV. The reconstructed mass  $m_t^{\text{rec}}$  is extracted from the  $\chi^2$  fit.

The fit above assumes the knowledge that a given jet comes from a  $b$  quark or a  $W$ -daughter quark in the final state. This knowledge is not available in principle, and thus one has to try all 12 possible jet-parton assignments. The number of combinations is reduced if one of the four highest  $E_T$  jet is  $b$ -tagged; it is then automatically assigned to a  $b$ -quark in the fitter. The number of jet-parton assignment is reduced to 6 and 2 when 1- and 2-tag are available, respectively. Masses of 5 and 0.5 GeV/ $c^2$  are assigned to the four-vectors of  $b$ -jets and  $W$ -daughter jets, respectively. There is an additional combination due to the 2 solutions for the  $p_z$  of the neutrino arising from solving a quadratic equation. After minimization of the  $\chi^2$  expression, the  $m_t^{\text{rec}}$  corresponding to the combination that yields the lowest  $\chi^2$  is considered the reconstructed top quark

mass for that event. An additional requirement of  $\chi_{\min}^2 < 9$  is found to give the best expected statistical uncertainty on the top mass (which is effective to reject badly reconstructed  $t\bar{t}$  events or background events). The efficiency for that cut decreases with the number of  $b$ -tags (since the number of available combinations is reduced) and ranges from 65% (38%) for 2-tag events to 91% (83%) for 0-tag events for signal (background) events. The number of events observed after the  $\chi^2$  cut are given in Table 1.

A typical reconstructed top mass distribution for signal Monte Carlo (for  $M_{\text{top}} = 178 \text{ GeV}/c^2$ ,  $\text{JES} = 0$ ) is shown in Fig. 2. The blue histogram in the same figure shows the case for the correct jet-parton assignment. The fraction of correct assignments increases with the number of  $b$ -tags as expected. Since the resolution of the reconstructed mass is dominated by the incorrect combinations, the  $m_t^{\text{rec}}$  resolution improves with the number of  $b$ -tags.

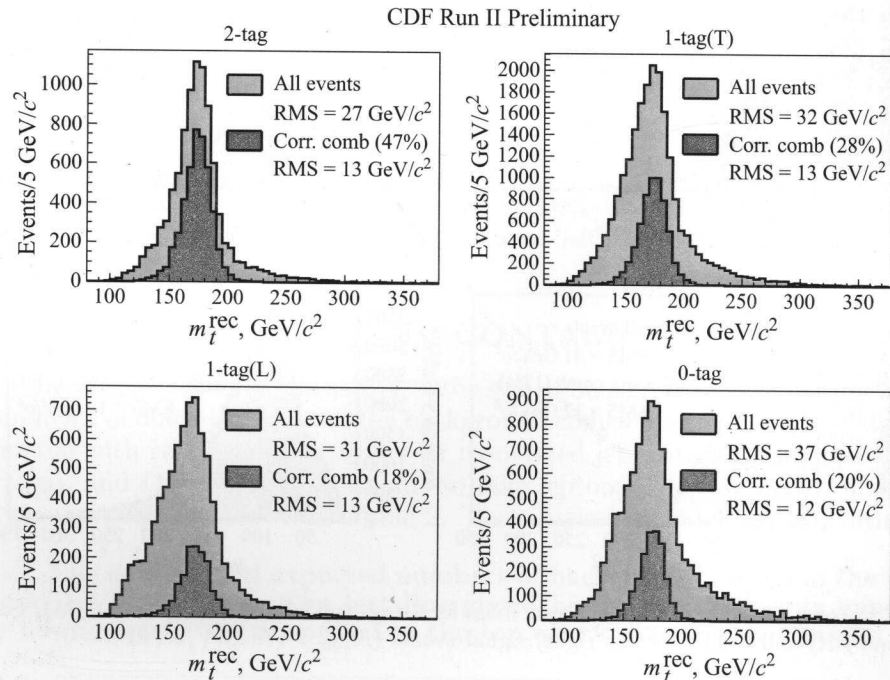


Fig. 2. Reconstructed top quark mass for 2-tag (top left), 1-tag(T) (top right), 1-tag(L) (bottom left) and 0-tag (bottom right) signal events ( $M_{\text{top}} = 178 \text{ GeV}/c^2$ ,  $\text{JES} = 0$ )

## 5. W BOSON MASS RECONSTRUCTION

The dijet mass from hadronic  $W$  boson decay  $m_{jj}$  is sensitive to the jet energy scale but is relatively insensitive to the true top quark mass. It can thus be used to determine fully *in situ* the jet energy scale with little uncertainty on  $M_{\text{top}}$ . In this analysis, the jet energy scale is determined using both the  $m_{jj}$  templates and the *a priori* determination of JES described in Sec. 3. The combination of both estimates provides an optimal constraint on this parameter.

The same jet corrections described in Sec.4 are applied to reconstruct  $m_{jj}$ . However, no  $\chi^2$  fitter is used and  $m_{jj}$  is simply reconstructed from the measured three-momenta of jets. A similar combinatorics problem to the  $m_t^{\text{rec}}$  reconstruction exists and is dealt with by considering all jet-parton assignments made of the four highest  $E_T$  jets that are not  $b$ -tagged. Consequently, there can be more than one mass per event that are considered. There are in fact 1, 3, and 6  $m_{jj}$  per event for the 2-tag, 1-tag and 0-tag subsamples, respectively. This reconstruction technique has been developed to optimize the sensitivity of  $m_{jj}$  to JES. A typical distributions of  $m_{jj}$  are shown in Fig. 3 for each event category (for  $M_{\text{top}} = 178 \text{ GeV}/c^2$ ,  $\text{JES} = 0$ ).

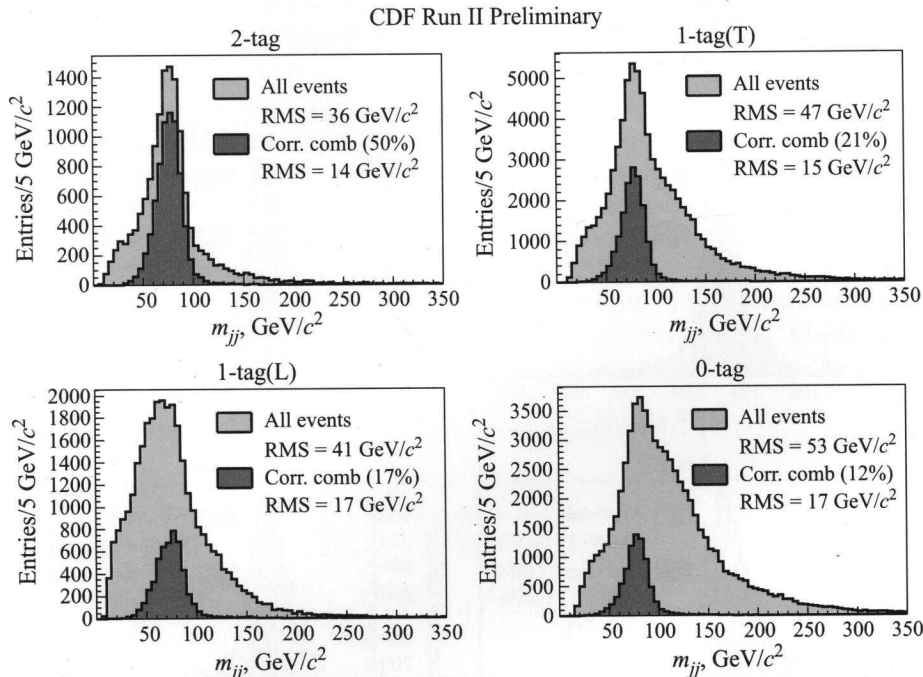


Fig. 3. Reconstructed hadronic  $W$  boson mass for 2-tag (top left), 1-tag(T) (top right), 1-tag(L) (bottom left) and 0-tag (bottom right) signal events ( $M_{\text{top}} = 178 \text{ GeV}/c^2$ ,  $\text{JES} = 0$ )

## 6. TOP AND $W$ MASS TEMPLATES FOR SIGNAL

Distributions of  $m_t^{\text{rec}}$  and  $m_{jj}$  are constructed from HERWIG  $t\bar{t}$  Monte Carlo for  $M_{\text{top}}$  values varying from 130 to 230  $\text{GeV}/c^2$  and JES values varying from  $-3$  to  $+3\sigma$ . Smooth probability density functions ( $P_{\text{sig}}(m_t^{\text{rec}} : M_{\text{top}}, \text{JES})$  and  $P_{\text{sig}}(m_{jj} : M_{\text{top}}, \text{JES})$ ) are obtained by fitting the mass distributions as a function of  $M_{\text{top}}$  and JES using an analytical function (the same is used for  $m_t^{\text{rec}}$  and  $m_{jj}$ : two Gaussian functions and one integrand of a gamma function) whose parameters depend linearly on each of these two parameters. Figure 4 shows the reconstructed top quark mass distribution for various true top quark mass (JES fixed at 0) for the 1-tag(T) subsample (left plot). Also in Fig. 4 is shown the  $m_{jj}$

distribution for various jet energy scale values ( $M_{\text{top}}$  fixed at  $175 \text{ GeV}/c^2$ ) for the 2-tag subsample (right plot). In both figures, the resulting fit is overlaid on the function, demonstrating the choice of function and dependence on  $M_{\text{top}}$  and JES are satisfying.

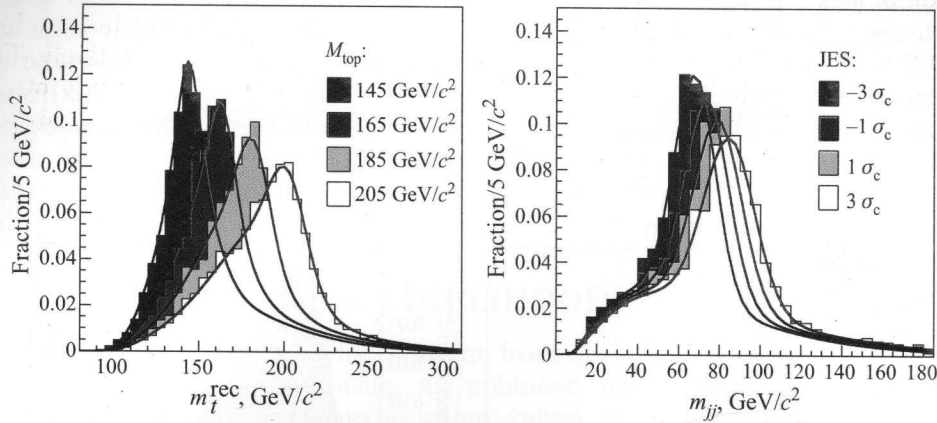


Fig. 4. Left plot: Signal  $m_t^{\text{rec}}$  templates are shown with top quark masses ranging from 145 to 205  $\text{GeV}/c^2$  and with JES set to 0 for the 1-tag(T) subsample. Right plot: Signal  $m_{jj}$  for JES values ranging from  $-3\sigma$  to  $+3\sigma$ , with  $M_{\text{top}}$  set to  $175 \text{ GeV}/c^2$  for the 2-tag subsample. Overlaid are the fitted parameterizations at each generated mass (left plot) and JES (right plot)

## 7. BACKGROUND CONTAMINATION

In the tagged lepton + jets samples, the size of backgrounds is small due to the requirement of one  $b$ -jet. Most of the background comes from  $W$  boson production associated with real heavy flavor jets, or associated jets with a misidentified  $b$ -jet (mistags), and QCD backgrounds due to fake leptons. The expected number of background events is shown in Table 2. There exists currently no quantitative

Table 2. The sources and expected numbers of background events in the three subsamples with  $b$  tags. The last line gives the number of events expected after the cut on  $\chi^2 < 9.0$ , applied in the top quark mass reconstruction

Source	Expected background		
	2-tag	1-tag(T)	1-tag(L)
$W$ + light jets	$0.40 \pm 0.08$	$3.22 \pm 0.41$	$4.14 \pm 0.53$
$Wb\bar{b} + Wc\bar{c} + Wc$	$1.12 \pm 0.43$	$3.91 \pm 1.23$	$6.81 \pm 1.85$
$WW/WZ$	$0.05 \pm 0.01$	$0.45 \pm 0.10$	$0.71 \pm 0.13$
non- $W$ (QCD)	$0.31 \pm 0.08$	$2.32 \pm 0.50$	$2.04 \pm 0.54$
Single top	$0.008 \pm 0.002$	$0.49 \pm 0.09$	$0.60 \pm 0.11$
Total	$1.89 \pm 0.52$	$10.4 \pm 1.72$	$14.3 \pm 2.45$
Total, $\chi^2 < 9.0$	$0.71 \pm 0.18$	$7.64 \pm 1.24$	$10.2 \pm 1.71$

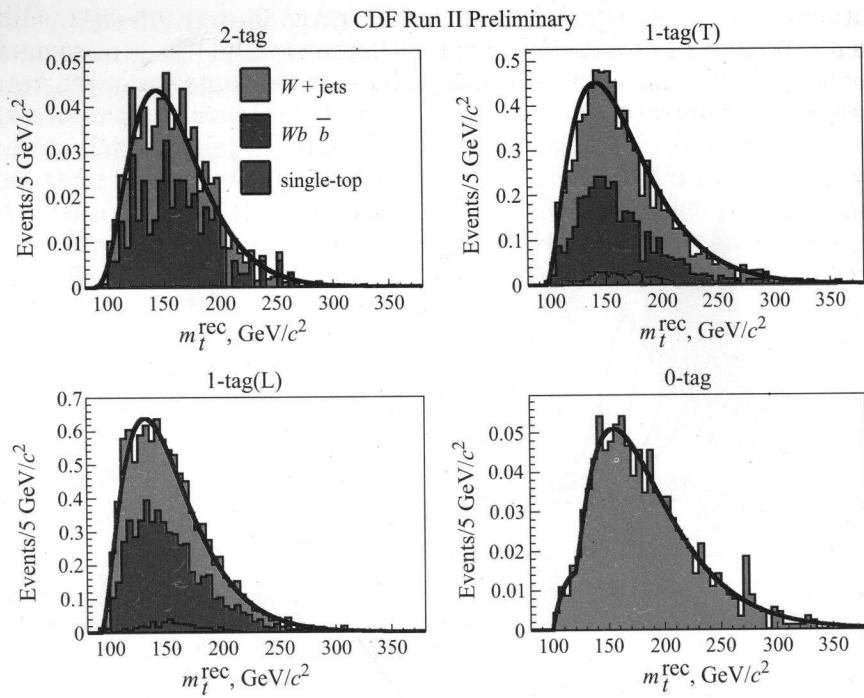


Fig. 5. Combined background  $m_t^{\text{rec}}$  templates for 2-tag events (top left), 1-tag(T) events (top right), 1-tag(L) events (bottom left) and 0-tag events (bottom right)

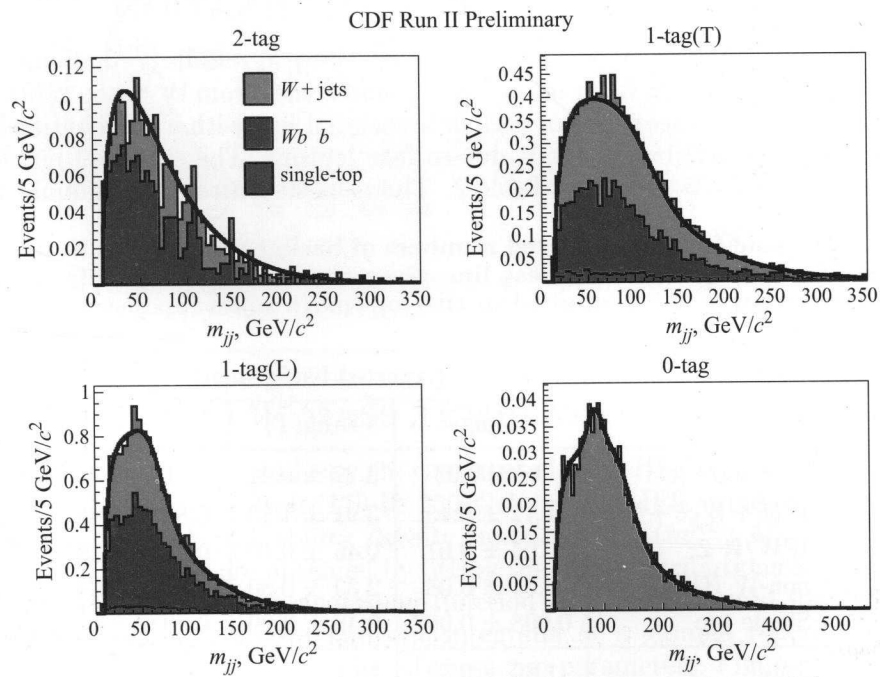


Fig. 6. Combined background  $m_{jj}$  templates for 2-tag events (top left), 1-tag(T) events (top right), 1-tag(L) events (bottom left) and 0-tag events (bottom right)

calculation of the background contamination in the 0-tag subsample, although studies have demonstrated the dominant background to be  $W + \text{jets}$  events which are modeled by the ALPGEN with HERWIG shower Monte Carlo generator.

Background templates for the  $W + \text{jets}$  with heavy flavor production and mistag cases are reconstructed using the ALPGEN [7] Monte Carlo samples. The mass template from QCD backgrounds with a fake lepton (extracted from the nonisolated lepton data) shows a very similar shape to the  $W + \text{jet}$  Monte Carlo (mistag) template. Thus, the mistag template is also used for the QCD background template. The combined  $m_t^{\text{rec}}$  and  $m_{jj}$  background templates are shown, respectively, in Figs. 5 and 6, as is the fitted curve to the template. Note that probability density functions for background events do not depend on  $M_{\text{top}}$  and JES\*.

## 8. LIKELIHOOD

The reconstructed mass distributions from data are compared to the signal and background templates using an unbinned likelihood fit. The likelihood involves parameters for the expectation values of the number of signal and background events in each subsample, and for the true top quark pole mass and jet energy scale. For each subsample, the likelihood is given by:

$$\mathcal{L}_{\text{sample}} = \mathcal{L}_{\text{shape}}^{m_t^{\text{rec}}} \times \mathcal{L}_{\text{shape}}^{m_{jj}} \times \mathcal{L}_{\text{nev}} \times \mathcal{L}_{bg}, \quad (2)$$

where

$$\begin{aligned} \mathcal{L}_{\text{shape}}^{m_t^{\text{rec}}} &= \prod_{k=1}^{r^W} \frac{\varepsilon_s n_s^W P_s(m_k^t; M_{\text{top}}, \text{JES}) + \varepsilon_b n_b^W P_b(m_k^t)}{\varepsilon_s n_s^W + \varepsilon_b n_b^W}, \\ \mathcal{L}_{\text{shape}}^{m_{jj}} &= \prod_{k=1}^{r^W \cdot n_i^c} \frac{n_s^W P_s(m_k^{jj}; M_{\text{top}}, \text{JES}) + n_b^W P_b(m_k^{jj})}{n_s^W + n_b^W}, \\ \mathcal{L}_{\text{nev}} &= \sum_{r_s^W + r_b^W = r^W} P_{\text{Pois}}(r_s^W; n_s^W) P_{\text{Pois}}(r_b^W; n_b^W) \times \\ &\quad \times \left[ \sum_{\substack{r_{s,b}^t \leq r_{s,b}^W \\ r_s^t + r_b^t = r^t}} P_{\text{Bin}}(r_s^t; r_s^W, \varepsilon_s) P_{\text{Bin}}(r_b^t; r_b^W, \varepsilon_b) \right]; \\ \mathcal{L}_{bg} &= \exp \left( -\frac{(n_b^W - n_b^W(\text{const}))^2}{2\sigma_{n_b^W}^2} \right). \end{aligned} \quad (3)$$

The most information on the true top quark mass is provided by the products in  $\mathcal{L}_{\text{shape}}^{m_t^{\text{rec}}}$ , the  $i$ th term of which gives the probability of observing the  $i$ th data

\* The dependence of the background templates to JES is very small and has been shown to have a negligible impact on the fitted top quark mass.

event with reconstructed mass  $m_i$ , given the background template,  $P_b(m_i)$ , and the signal template with a true top quark mass of  $M_{\text{top}}$  and energy scale shift JES,  $P_s(m_i, M_{\text{top}}, \text{JES})$ . The third term represents the information arising from the number of signal and background events in the top quark mass and dijet mass samples, which are correlated. We denote the number of expected signal and background events in the  $W \rightarrow jj$  sample,  $n_s^W$  and  $n_b^W$ , respectively. The expected numbers of signal and background events in the  $m_t^{\text{rec}}$  sample are given by  $\varepsilon_s n_s^W$  and  $\varepsilon_b n_b^W$ , respectively, where the two parameters  $\varepsilon_s$  and  $\varepsilon_b$  represent the efficiency of the  $\chi^2$  cut for signal and background events. The third term in the likelihood,  $\mathcal{L}_{\text{nev}}$ , expresses the likelihood associated with observing  $r_W$  and  $r_t$  events in the two samples given the expected number of events and the expected efficiencies. The first sum expresses the Poisson probability to observe  $r_s^W$  signal and  $r_b^W$  background events given Poisson means of  $n_s^W$  and  $n_b^W$ , respectively. The sum in the third term is over the sum of those signal and background events that equal the observed number of events in the  $m_{jj}$  sample:  $r_s^W + r_b^W = r^W$ . For each pair in this sum, we then include the binomial probability to observe  $r_s^t$  signal events and  $r_b^t$  background events in the  $m_t^{\text{rec}}$  sample given the numbers of observed events in the  $m_{jj}$  sample and the  $\chi_{\text{min}}^2$  cut efficiencies. The second sum in the  $\mathcal{L}_{\text{nev}}$  is over the pairs of signal and background events in the  $m_t^{\text{rec}}$  sample that equal to the observed number of events:  $r_s^t + r_b^t = r^t$ .

When independent estimates of background are available, the background normalizations are constrained in the likelihood fit by Gaussian terms with the form of  $\mathcal{L}_{bg}$ . The background normalizations are constrained for the 2-tag, 1-tag(T), and 1-tag(L) samples. Both  $n_s$  and  $n_b$  are required to be greater than zero. The *a priori* constraint on the jet energy scale described in Sec. 3 is used in the likelihood under the form of a Gaussian constraint:

$$\mathcal{L}_{\text{JES}} = e^{-\frac{(\text{JES} - \text{JES}^{\text{exp}})^2}{2\sigma_{\text{JES}}^2}}, \quad (4)$$

$$= e^{-\frac{\text{JES}^2}{2}}, \quad (5)$$

where the simplification arises because by definition the measured shift in energy scale,  $\text{JES}^{\text{exp}} = 0$  and the uncertainty  $\sigma_{\text{JES}} = 1.0$ .

The total likelihood is given by the product of the likelihoods for the four subsamples and the jet energy scale constraint:

$$\mathcal{L} = \mathcal{L}_{2\text{-tag}} \times \mathcal{L}_{1\text{-tag(T)}} \times \mathcal{L}_{1\text{-tag(L)}} \times \mathcal{L}_{0\text{-tag}} \times \mathcal{L}_{\text{JES}}. \quad (6)$$

The true top quark mass  $M_{\text{top}}$  and jet energy scale JES are shared between the four likelihoods and are free parameters in the fit. The likelihood is maximized with respect to all ten parameters ( $n_s$  and  $n_b$  for four subsamples, JES, and  $M_{\text{top}}$ ).

The likelihood procedure is tested by performing pseudo-experiments in which for the pseudo-data the  $m_t^{\text{rec}}$  and  $m_{jj}$  are generated randomly from the Monte Carlo distributions corresponding to various values  $M_{\text{top}}$  and JES. In Fig. 7 are shown the mean and width of the pull distributions for various values of  $M_{\text{top}}$  and JES. The central values and uncertainties are well behaved for large

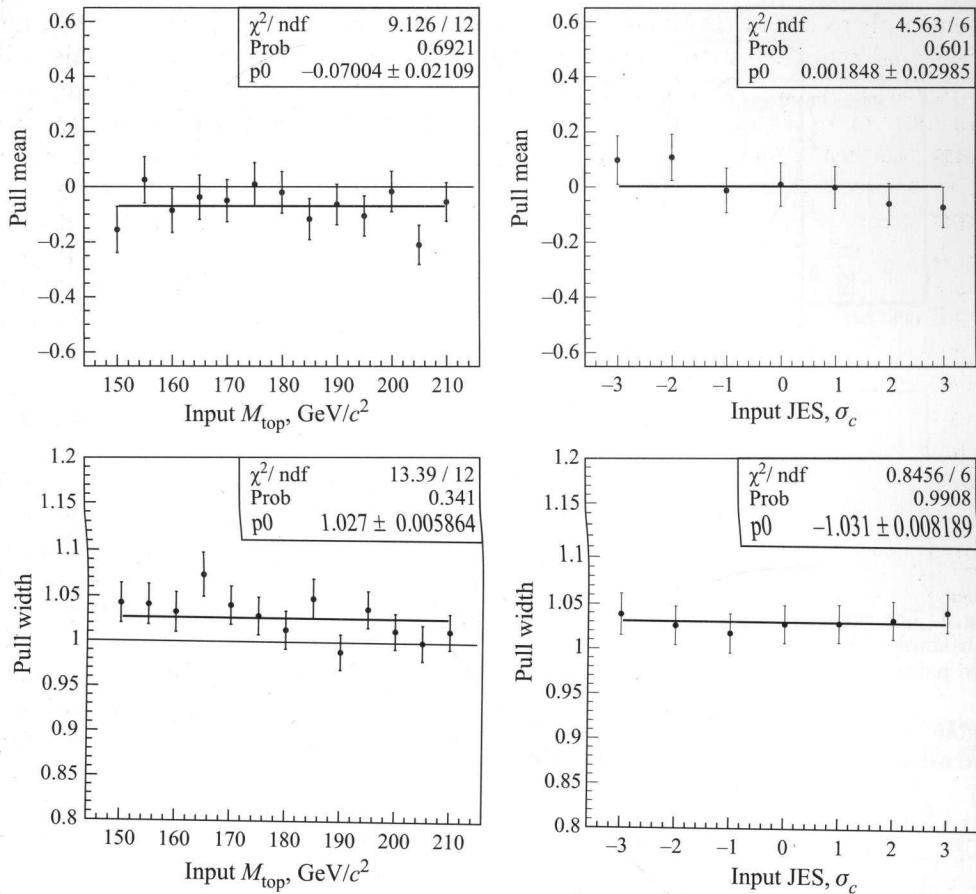


Fig. 7. The mean (top) and width (bottom) of pull distributions from sets of 2500 pseudo-experiments are shown. On the left, the jet energy scale is fixed at its nominal value, and the generated top quark mass is varied from 150 to 210  $\text{GeV}/c^2$ . On the right, the top quark mass is fixed at 175  $\text{GeV}/c^2$ , and the input jet energy scale is varied from  $-3\sigma$  to  $+3\sigma$ . The error bars come mostly from the limited statistics of the Monte Carlo samples from which the pseudo-data is taken

ranges of  $M_{\text{top}}$  and JES. The pull width as a function of  $M_{\text{top}}$  are slightly larger than one: 1.027. The uncertainties obtained in the data are scaled by that factor to guarantee 68% coverage of the  $1\sigma$  uncertainties. The mean of the pull distributions are modestly biased on average ( $-0.3 \text{ GeV}/c^2$ ) and this value is included as a systematic uncertainty (see Sec. 10).

## 9. RESULTS

The likelihood procedure is then applied to the data events. The result is a top quark mass of  $173.5^{+3.7}_{-3.6}(\text{stat.} + \text{JES}) \text{ GeV}/c^2$ . The simultaneous measurement of the jet energy scale is  $-0.10^{+0.78}_{-0.80}\sigma$ . The combined likelihood as a function of the true top quark mass and JES is shown in Fig. 8.

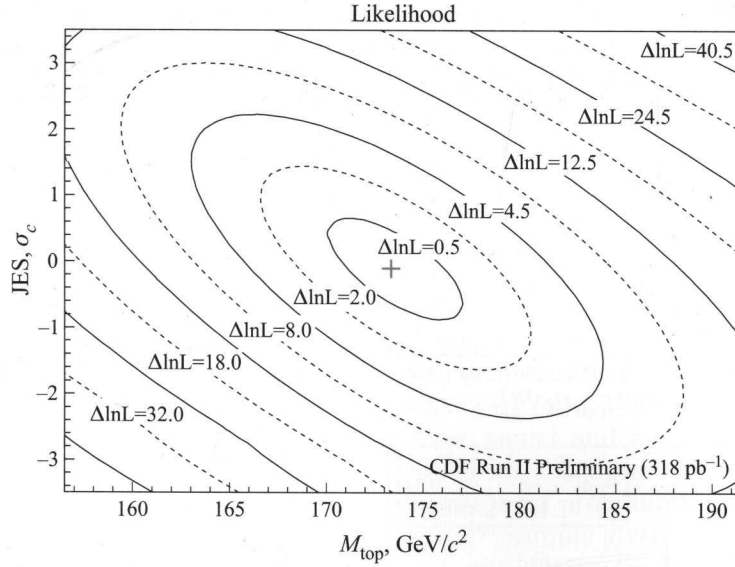


Fig. 8. The contours of the likelihood in the  $M_{\text{top}} - \text{JES}$  plane for the combined fit to all four subsamples. At each point in the plane, the likelihood is maximized with respect to the other free parameters. The cross-hair shows the best fit point

Table 3. The input constraints and fitted values are given for all free parameters in the combined likelihood fit

Category	2-tag	1-tag(T)	1-tag(L)	0-tag
$M_{\text{top}}$		$173.5^{+3.7}_{-3.6} (\text{stat.} + \text{JES}) \text{ GeV}/c^2$ $(173.5^{+2.7}_{-2.6} (\text{stat.}) \pm 2.5 (\text{JES}) \text{ GeV}/c^2)$		
JES		$-0.10^{+0.78}_{-0.80} \sigma$		
$n_s$	$23.5 \pm 5.0$	$53.9 \pm 7.9$	$14.3 \pm 5.2$	$28.3 \pm 8.3$
$n_b$	$1.8 \pm 0.5$	$10.1 \pm 1.7$	$15.5 \pm 2.2$	$15.7^{+8.0}_{-7.1}$

The uncertainty on  $M_{\text{top}}$  from the likelihood fit is a combination of the statistical uncertainty in extracting a measurement of  $M_{\text{top}}$  and the systematic uncertainty due to allowed variations of JES. It is possible to get an idea of the size of each contribution. Fixing JES to its fitted value of  $-0.10\sigma$  and fitting for  $M_{\text{top}}$  alone yields a top quark mass measurement of  $173.5^{+2.7}_{-2.6} (\text{stat.} + \text{JES}) \text{ GeV}/c^2$ , corresponding to the «pure statistical» uncertainty. Subtracting this uncertainty in quadrature from the full uncertainty gives an  $M_{\text{top}}$  uncertainty due to the jet energy scale of  $\pm 2.5 \text{ GeV}/c^2$ .

The input constraints and fit results for the combined fit are given in Table 3. Figure 9 shows the consistency of the reconstructed top quark mass distribution in each subsample with the combined fit results, while Fig. 10 shows the same for the  $m_{jj}$  distributions.

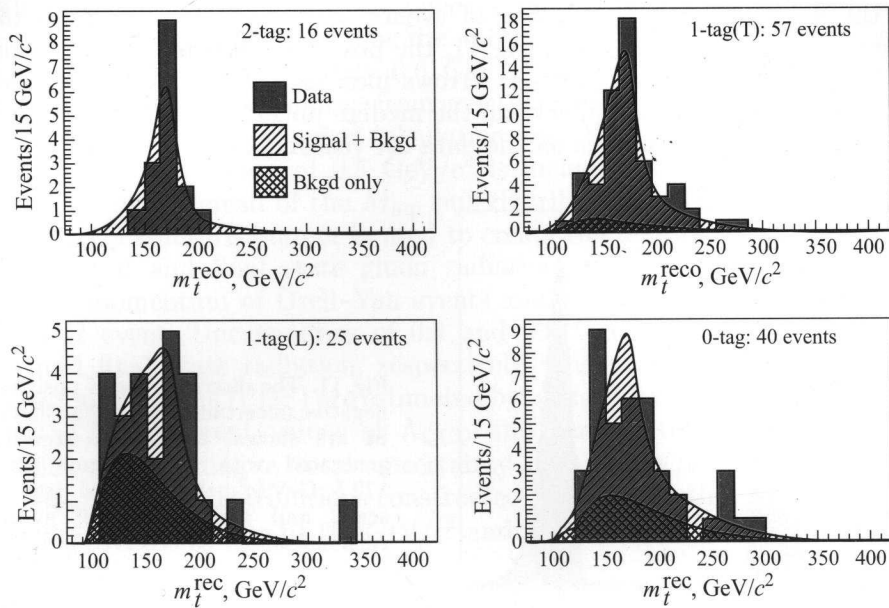


Fig. 9. The reconstructed top quark mass distribution for each subsample is shown overlaid with the expected distribution using the top mass, jet energy scale, signal normalization, and background normalization from the combined fit

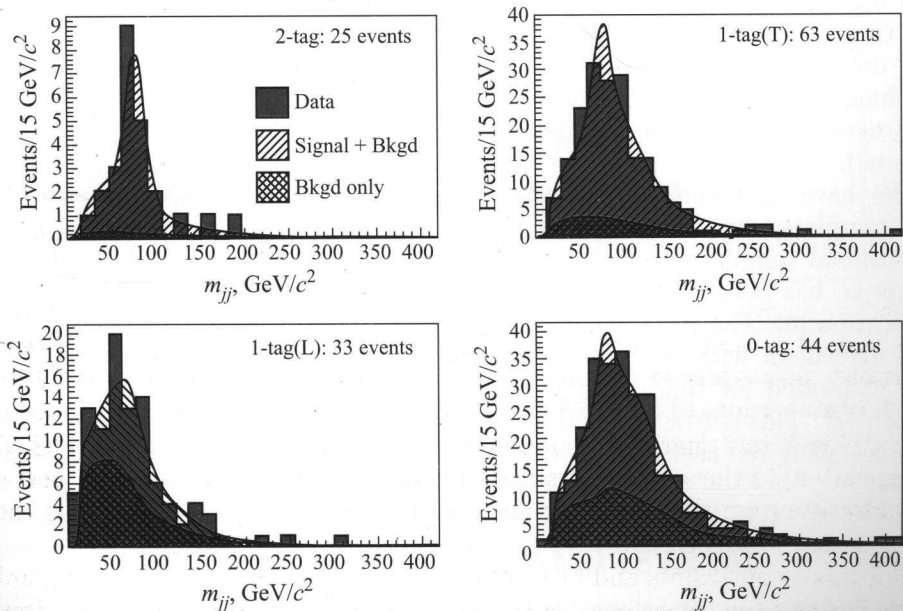


Fig. 10. The reconstructed dijet mass distribution for each subsample is shown overlaid with the expected distribution using the top mass, jet energy scale, signal normalization, and background normalization from the combined fit

A set of pseudo-experiments is generated with a true top quark mass of  $172.5 \text{ GeV}/c^2$  and the nominal jet energy scale (both close to the central value from the fit) and with the number of events in each subsample equal to the number observed in our data. In Fig. 11, the positive and negative uncertainties from the likelihood fits are plotted. Arrows indicate the uncertainties from the fit to the data. Although smaller than the median uncertainties from the pseudo-experiments, the uncertainties on the data are reasonable.

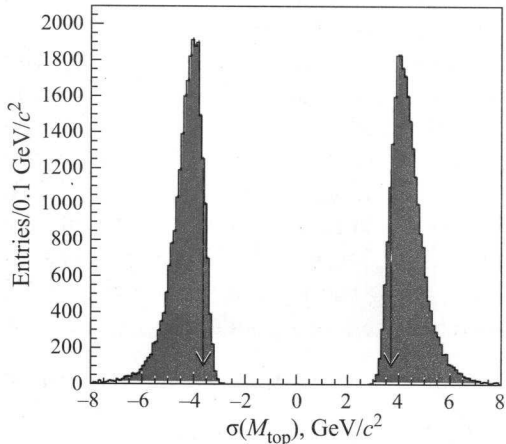


Fig. 11. The distributions of positive and negative uncertainties from the likelihood fit are shown, for pseudo-experiments generated with a true top mass of  $172.5 \text{ GeV}/c^2$ , the nominal jet energy scale, and the number of events in each subsample as observed in the data. Arrows indicate the positive and negative uncertainties from the likelihood fit to the data.

**Alternate Fits.** More fits to the data have been performed with some variations to the default procedure to verify the robustness of the result. One test is to remove the JES *a priori* constraint (i.e. the term  $\mathcal{L}_{\text{JES}}$  in Eq. 4) to check that the fit of the jet energy scale from  $W \rightarrow jj$  only is consistent with the prior CDF determination. The result of the fit is  $174.0 \pm 4.5(\text{stat.} + \text{JES}) \text{ GeV}/c^2$  with the simultaneous fit of JES yielding  $-0.25 \pm 1.22(\text{stat.})\sigma$ . The results are in very good agreement with the primary result, although with larger uncertainties as expected.

We have also performed a «traditional» template analysis in which only  $m_t^{\text{rec}}$  templates are considered and the JES is not a parameter of the fit (one-dimensional template analysis). This constitutes a good cross-check since that technique has been widely used in the past, for instance, for the Run I CDF publication [6]. The resulting fitted  $M_{\text{top}} = 173.2 \pm 2.9(\text{stat.}) \text{ GeV}/c^2$ , is in very good agreement with the primary result. The jet energy scale uncertainties have been estimated for that analysis from the CDF prior determination and yield  $3.1 \text{ GeV}/c^2$ . This is 20% larger than for the primary result ( $2.5 \text{ GeV}/c^2$ ), therefore demonstrating the usefulness of the  $W \rightarrow jj$  calibration already with the current dataset.

## 10. SYSTEMATIC UNCERTAINTIES

Various sources of uncertainties are considered for this measurement, apart from the jet energy scale that is given from the fit. The estimate of the jet energy scale from *a priori* information (described in Sec. 3) and from  $W \rightarrow jj$  decays

do not give direct information on the  $b$ -jets energy scale. The  $b$ -jets can behave differently than gluon and light quark jets because of their different fragmentation models, more abundant semileptonic decays and different color flow in  $t\bar{t}$  events than  $W$ -daughter jets. We find that the uncertainties due to the unique features of the  $b$ -jet are quite small, only  $0.6 \text{ GeV}/c^2$  in total, thus most of the  $b$ -jet uncertainty is due to uncertainties from generic jet energy scale that is determined in this analysis from the *a priori* calculation and  $W \rightarrow jj$  decays.

A method uncertainty of  $0.5 \text{ GeV}/c^2$  is included to account for the small average bias in the mean of the  $M_{\text{top}}$  pull distributions (see Sec. 8) and for the fact that a constant JES factor is used to create the templates\*.

The initial and final state gluon radiation is estimated by studying the transverse momentum of Drell-Yan events and extrapolating the results to the  $Q^2$  of a  $t\bar{t}$  event. Uncertainties of  $0.4$  and  $0.6 \text{ GeV}/c^2$  are estimated for the initial and final state radiation, respectively. The uncertainties in the parton distribution functions (PDF) are estimated by using different PDF sets (CTEQ5L vs. MRST72), different values of  $\Lambda_{\text{QCD}}$  and varying the eigenvectors of the CTEQ6M set, yielding a total uncertainty of  $0.3 \text{ GeV}/c^2$ . The difference in fitted  $M_{\text{top}}$  for mass distributions constructed using the Pythia [8] and HERWIG generators is evaluated to be  $0.2 \text{ GeV}/c^2$  and is taken as a generator uncertainty.

Table 4. This table summarizes all systematic uncertainties for the combined analysis

Method	Primary		$M_{\text{top}}$ only
	$\Delta M_{\text{top}}, \text{ GeV}/c^2$	$\Delta \text{JES}(\sigma)$	$\Delta M_{\text{top}}, \text{ GeV}/c^2$
Jet energy	N/A	N/A	3.1
$b$ -jet energy	0.6	0.25	0.6
Method	0.5	0.02	N/A
ISR	0.4	0.08	0.4
FSR	0.6	0.06	0.4
PDFs	0.3	0.04	0.4
Generators	0.2	0.15	0.3
Background shape	0.5	0.08	0.5
$b$ -tagging	0.1	0.01	0.2
MC statistics	0.3	0.05	0.4
Total	1.3	0.33	3.3

The uncertainties in the background mass shape is dominated by the  $Q^2$  scale used in the generation of  $W$  + jets events. ALPGEN samples with various  $Q^2$  scales ( $4M_W^2$ ,  $M_W^2$ ,  $M_W^2/4$ , and  $M_W^2 + P_{TW}^2$ ) are used to extract different background mass templates that introduce an uncertainty of  $0.4 \text{ GeV}/c^2$ . A second, smaller contribution to this uncertainty is estimated by performing sets of pseudo-experiments in which background events are drawn not from the

\* The templates are created by shifting all jets in an event by the same JES factor. This does not correspond to reality in general, e.g. low- $p_T$  jets could suffer larger JES shift than high- $p_T$  jets.

combined background template but from templates for one of the individual background processes, including the templates derived from QCD-enriched data. These uncertainties are estimated to be  $0.3 \text{ GeV}/c^2$ .

The uncertainty in the MC modeling of the  $b$ -tagging efficiency as a function of jet  $p_T$  is evaluated to be  $0.1 \text{ GeV}/c^2$ . Finally, the uncertainty from the limited statistics available to create the Monte Carlo templates is evaluated to be  $0.3 \text{ GeV}/c^2$ .

The summary of the systematic uncertainties is given in Table 4. Also in Table 4 are shown the uncertainties on the fitted JES and for the traditional one-dimensional template analysis that is used as a cross-check. The uncertainties are assumed uncorrelated and added in quadrature to yield  $1.3 \text{ GeV}/c^2$  for the primary analysis.

## 11. CONCLUSION

We have measured the top quark mass to be  $173.5 \pm \frac{2.7}{2.6}(\text{stat.}) \pm \pm 2.8(\text{syst.}) \text{ GeV}/c^2$ , or equivalently

$$M_{\text{top}} = 173.5 \pm \frac{3.9}{3.8} \text{ GeV}/c^2$$

using  $318 \text{ pb}^{-1}$  of data collected by the CDF detector. The lepton + jets final state has been studied and a template technique employed to extract  $M_{\text{top}}$ . The dominant systematic uncertainty, the jet energy scale, has been reduced by using the *in situ* information from  $W \rightarrow jj$  decays. Two-dimensional templates of the reconstructed top quark and hadronic  $W$  boson mass have been used to extract simultaneously the true top quark mass and the jet energy scale. This two-dimensional analysis is used to take into account the correlations between

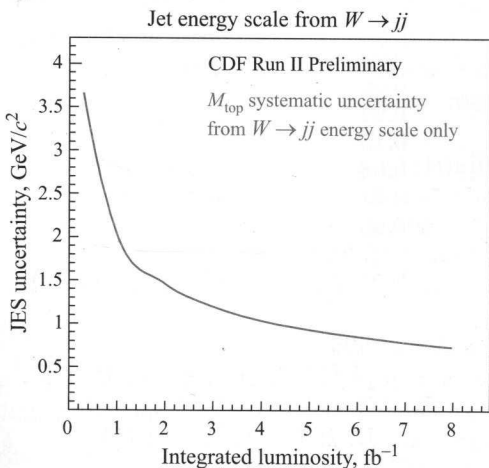


Fig. 12. Jet energy scale uncertainty from  $W \rightarrow jj$  calibration only as a function of integrated luminosity

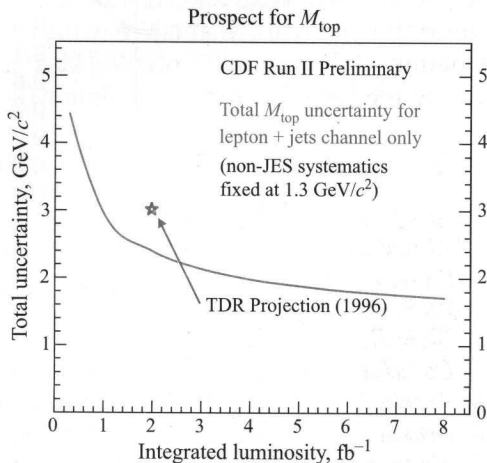


Fig. 13. Total  $M_{\text{top}}$  uncertainty as a function of integrated luminosity where the systematic uncertainties apart from JES are constant and equal to the current estimate. The projection of the CDF-II Technical Design Report [3] is indicated by a star

these two parameters. Cross-checks of the primary result have been performed, including a one-dimensional analysis similar to the Run I analysis [6], and yield consistent results.

We note that the jet energy scale uncertainty is expected to improve more data are available to perform the  $W \rightarrow jj$  calibration. Figure 12 shows the jet energy scale uncertainty using only the  $W \rightarrow jj$  information as a function of integrated luminosity. We can expect a JES uncertainty in the top quark mass measurement of approximately  $1 \text{ GeV}/c^2$  by the end of Run II. The projected total  $M_{\text{top}}$  uncertainty is shown in Fig. 13 as a function of integrated luminosity for Run II where the systematic uncertainties apart from JES are constant and equal to the current estimate ( $1.3 \text{ GeV}/c^2$ ). We note that this conservative estimate yields a better uncertainty than for the  $M_{\text{top}}$  uncertainty of  $3 \text{ GeV}/c^2$  for all channels projected in the CDF-II Technical Design Report [3] with  $\int \mathcal{L} dt = 2 \text{ fb}^{-1}$  (indicated on the plot). Our projection predicts that a top quark mass uncertainty of  $2 \text{ GeV}/c^2$  or better can be achieved by the end of Run II ( $\approx 4\text{--}8 \text{ fb}^{-1}$ ) only for one analysis in the lepton + jets channel.

**Acknowledgments.** We thank the Fermilab staff and the technical staffs of the participating institutions for their vital contributions. This work was supported by the U.S. Department of Energy and National Science Foundation; the Italian Istituto Nazionale di Fisica Nucleare; the Ministry of Education, Culture, Sports, Science and Technology of Japan; the Natural Sciences and Engineering Research Council of Canada; the National Science Council of the Republic of China; the Swiss National Science Foundation; the A.P. Sloan Foundation; the Bundesministerium fuer Bildung und Forschung, Germany; the Korean Science and Engineering Foundation and the Korean Research Foundation; the Particle Physics and Astronomy Research Council and the Royal Society, UK; the Russian Foundation for Basic Research; the Comision Interministerial de Ciencia y Tecnologia, Spain; and in part by the European Community's Human Potential Programme under contract HPRN-CT-20002, Probe for New Physics.

## References

1. Abe F. *et al.* // Phys. Rev. Lett. 1995. V. 74. P. 2626;  
Abachi S. *et al.* // Phys. Rev. Lett. 1995. V. 74. P. 2632.
2. Simmons E. // Proc. of Thinkshop on Top Quark Physics at Run II, Batavia, IL, 1998. hep-ph/9908511.
3. Blair R. *et al.* (CDF-II). PUB. 96-390-E. Fermilab, 1996.
4. Corcella G. *et al.* // JHEP. 2001. V. 01. P. 010. [hep-ph/0011263]; hep-ph/0210213.
5. Acosta D. *et al.* (CDF Collaboration) // Phys. Rev. D. 2005. V. 71. P. 052003.
6. Acosta D. *et al.* (CDF Collaboration) // Phys. Rev. D. 2001. V. 63. P. 032001.
7. Mangano M. L. *et al.* // J. High Energy Phys. 2003. V. 07. P. 001.
8. Sjostrand T. *et al.* // Comp. Phys. Commun. 2001. V. 135. P. 238.

Received on December 9, 2005.

Адельман Дж. и др. (по поручению коллаборации CDF) E1-2005-131  
Измерение массы топ-кварка методом шаблонов и калибровки струй  
по распаду  $W \rightarrow jj$  в событиях типа лептон + струи на CDF-II

Измерена масса топ-кварка в наборе событий типа лептон + струи в протон-антипротонных взаимодействиях при  $\sqrt{s} = 1,96$  ТэВ. Интегральная светимость данных составила  $318 \text{ пб}^{-1}$ , что позволило найти 138  $t\bar{t}$ -кандидатов в четырех различных поднаборах. Масса топ-кварка восстановлена для каждого события с помощью законов сохранения энергии и импульса. Также применялась связь на восстановление массы  $W$ -бозона из адронного распада на две струи для уменьшения систематической ошибки от энергетической калибровки калориметра. Смоделированы наборы шаблонов для различных значений масс топ-кварка и энергий струй. Распределение реконструированных масс топ-кварка и  $W$ -бозона, полученное из экспериментальных данных, сравнивалось с шаблонами Монте-Карло методом наибольшего правдоподобия. В результате получена масса топ-кварка  $M_{\text{top}} = 173,5_{-3,8}^{+3,9} \text{ ГэВ}/c^2$ . Этот результат является наиболее точным на сегодня.

Сообщение Объединенного института ядерных исследований. Дубна, 2005

Adelman J. et al. (On behalf of the CDF Collaboration) E1-2005-131  
Measurement of the Top Quark Mass Using the Template Method  
in the Lepton Plus Jets Channel with *in situ*  $W \rightarrow jj$  Calibration at CDF-II

We report on a measurement of the top quark mass in the lepton plus jets channel of  $t\bar{t}$  events from  $p\bar{p}$  collisions at  $\sqrt{s} = 1.96$  TeV. This measurement uses an integrated luminosity of  $318 \text{ pb}^{-1}$  data, which brings 138  $t\bar{t}$  candidates separated into four subsamples. A top quark mass is reconstructed for each event by using energy and momentum constraints on the top-quark pair decay products. We also employ the reconstructed mass of hadronic  $W$  boson decays  $W \rightarrow jj$  to constrain *in situ* the largest systematic uncertainty of the top quark mass measurement: the jet energy scale. Monte Carlo templates of the reconstructed top quark and  $W$  boson masses are produced as a function of the true top quark mass and the jet energy scale. The distribution of reconstructed top quark and  $W$  boson masses in the data are compared to the Monte Carlo templates using a likelihood fit to obtain:  $M_{\text{top}} = 173.5_{-3.8}^{+3.9} \text{ GeV}/c^2$ . This constitutes the most precise measurement of the top quark mass up to date.

Communication of the Joint Institute for Nuclear Research. Dubna, 2005